Influence of CdSe/ZnS Quantum Dots in the Polymerization Process and in the Grating Recording in Acrylate Materials

Anne Barichard,[†,‡,§] Tigran Galstian,[§] and Yaël Israëli*[,†,‡]

Clermont Université, Université Blaise Pascal, Laboratoire de Photochimie Moléculaire et Macromoléculaire, BP 10448, 63000 Clermont-Ferrand, France, CNRS, UMR 6505, Laboratoire de Photochimie Moléculaire et Macromoléculaire, 63177 Aubière, France, and Center of Optics, Photonics and Laser, Department of Physics, Engineering Physics and Optics, Laval University, 2375 rue de la Terrasse, Québec G1 V 0A6, Canada

Received: May 4, 2010; Revised Manuscript Received: October 1, 2010

The initiation step of the polymerization of acrylate materials is first studied in detail by UV−visible spectroscopy, showing the involvement of each species of the three-component photosensitizer. Then, the implementation of a combined holographic and physicochemical investigation approach is used to determine the influence of photoluminescent CdSe/ZnS quantum dots (QDs) in the photopolymerization and grating recording process in composites containing those QD nanoparticles. The fluorescence microscopy evidences the dynamic distribution profile of QDs due to their diffusion from the irradiated zones to the interface between the bright and the dark zones and, finally, their accumulation in nonirradiated zones. At the same time, the infrared spectroscopy shows that the presence of QDs provides a noticeable decrease of the polymerization rate, which favors the diffusion of the monomer and QDs. These two phenomena contribute to the enhancement of the refractive index modulation depth.

Introduction

Various emerging applications of holography in data storage, sensors, authentication security technologies, optical devices, optical fiber communications, or lasers[1−6] required the development of advanced polymer materials. Photopolymerizable compositions played an important role in this material development since those are materials with high sensitivity, low cost, and easy (self) processability. Since the past decade, to increase the refractive index modulation depth (difference between the bright and dark regions of the light grating), many studies were conducted in nanoparticle-dispersed polymers,[7] such as luminescent inorganic nanoparticles,[7−9] gold,[10,11] silver,[12] polystyrene latex spheres,[11] silicate clay powder,[11] TiO_2,[7,13−16] SiO_2,[7,16−19] ZrO_2,[20,21] and Si-MFI zeolite or zeolite beta nanoparticles.[22,23] In order to introduce the nanoparticles into the monomer mixtures, surface modification was a general approach.[7,24−26]

Most holographic mixtures were composed of two acrylate monomers; however, Tomita's group usually used a one-monomer system.[14,27] To understand the origins of the increase of the refractive index modulation depth of the gratings recorded in such a nanoparticle-dispersed photopolymer, a mechanism was proposed using the chemical potential of each constituent.[28] Indeed, under exposure, the polymerization provoked an imbalance of the components (in the illuminated zones versus dark zones) and therefore disturbed the thermodynamic equilibrium of the system. This triggered the migration of the monomers from the dark to the bright regions. The nanoparticles underwent a counter diffusion. This latter process was favored by the monofunctional monomer.[14] Such process gave rise to the formation of a grating patterning with a spatial distribution of nanoparticles. Optical-phase shift measurement, transmission electron microscopy, scanning electron microscopy, Raman and confocal Raman microscopy, electron probe microanalyzer analysis, atomic force microscopy, and fluorescence microscopy evidenced the nanoparticle separation in the interference pattern.[7,8,10,12,14,16,18−23,26,29] It is worthy to note that the counter diffusion of nanoparticles could occur only if the diffusion process of the nanoparticle was not prevented. Indeed, in studies on a photopolymerizable mixture containing surface-photoreactive SiO_2 nanoparticles, Park et al. pointed out that the high diffraction efficiency (near 90%) could not be explained by the simple counter diffusion process. In this system, the surface-photoreactive SiO_2 was a comonomer, and in this case, their diffusion was impossible. The diffraction efficiency enhancement there was attributed to an interfacial polarity change via the hydrogen bonding induced between the hydroxyl group at the surface of SiO_2 and the polar constituents of the photopolymer.[30,31] The diffusion of the monomers depended on the cross-link density; the higher the latter, the lower the diffusion. To reduce the cross-link density, Park and co-workers have recently developed a new photopolymer system formed of inorganic−organic hybrid interpenetrating networks.[32] They demonstrated that the interpenetrated hard inorganic networks were uniformly distributed within the soft organic networks. This feature led to the low cross-link density of the organic networks, which allowed the fast monomer diffusion and thus higher diffraction efficiency.[32] For most of the photopolymer and nanoparticle-dispersed material systems, an induction period was observed at the initial stage of recording. This feature was ascribed to the presence of oxygen, which could inhibit the polymerization. Yao et al. have demonstrated that the introduction of thiol in the nanoparticle-dispersed monomer mixture not only reduced the inhibition period but also improved the diffraction efficiency and the recording sensitivity.[33]

Recently, we have been involved in the study of an acrylate photopolymer composition that was doped with CdSe/ZnS quantum dots (QDs).[34] The fluorescence property of QDs was

* To whom correspondence should be addressed. E-mail: yael.israeli@univ-bpclermont.fr.
† Université Blaise Pascal.
‡ CNRS.
§ Laval University.

10.1021/jp1040713
Published on Web 11/01/2010

used as a probe to directly evidence the photoinduced diffusion of QDs in the photopolymerizable mixture. For this purpose, a spatially nonuniform "one line intensity" exposition was used (using a cylindrical lens). It was observed that the position of the minimum of photoluminescence and of the maximum value of the laser intensity were identical. In addition and most importantly, the maximum of the photoluminescence of QDs was observed at the maximum of the gradient of the recording beam's intensity. Such results highlighted the diffusion of the QDs upon heterogeneous exposure,[34] as observed in the case of nanoparticle-dispersed photopolymers. The formation of these nanostructured materials could be interesting for many applications, including active bar codes, distributed feedback lasing devices, the tuning of the lasing wavelength, and the dimensional morphology of the laser resonators.[7]

Since, a one line intensity exposition demonstrated a diffusion of the QDs, the next step was to examine the influence of QDs on the diffraction efficiency and therefore in the refractive index modulation depth. To this end, in the present work, gratings were recorded in pure monomer mixture and in a QD dispersed photopolymerizable mixture. First, particular attention was given to the mechanism of initiation of the photopolymerization involving a three-component sensitizer composed of dye, amine, and tetrabromomethane. Then, a combined holographic and photochemical study approach was applied in order to have better insight into reactions involved during the hologram formation. Particular attention was paid to the involvement of QDs in the polymerization process. For this purpose, we studied the fate of the photosensitizer and the monomers by UV−visible and infrared spectroscopy in the absence and in the presence of QDs to determine the participation of the nanoparticles in the photopolymerization process.

Experimental Section

Materials. The acrylate monomers, dipentaerithritol pentaacrylate (DPEPA) and 2(2-ethoxyethoxy)ethyl acryalte (2EEEA) were purchased from Aldrich and were used as received without further purification. The QDs (5.2 nm diameter) were supplied (in toluene) by Nanoco Technologies. Those are nanoparticles with a CdSe core and ZnS shell. The extraction of QDs was performed by precipitation in isopropanol under strong centrifugation.

The basic syrup for photopolymerization was prepared in the absence of light by mixing the acrylate monomer (80:20 DPEPA/2EEEA) with the three-component initiator. This latter included eosin Y (0.3 wt %) as a light-absorbing agent, ethyl 4-dimethylaminobenzoate (EDMABzt 4.0 wt %), as an electron donor, and the third component CBr_4 (5.8 wt %), which took part in the polymerization process.[35] Dried QDs (0.5 or 1 wt %) were then added in the syrup, and the dispersion was performed by using a magnetic stirrer for a day.

To form the optical cell, the syrup (with or without QDs) was sandwiched between two glass slides separated by an 11 μm thick aluminum film used as a spacer.

Experimental Setup and Procedure. The sample cell, filled either with the monomer syrup only or with the QDs dispersed in the monomer syrup, was exposed to a normally incident photopolymerizing laser beam, obtained from a diode laser (Spectra) operating at 488 nm. A lens was used to increase the laser spot to a dimension of 1 cm^2 on the position of the sample. Different laser intensities, measured at the position of the sample (by a photodiode, from Gentec) and ranging from 10 to 40 mW cm^{-2} (limited by the maximum power delivered by the laser), were used during the experiments. The periodic (grating-like) pattern was recorded through an amplitude mask with a fringe spacing of 100 μm (50% fill factor). The mask was positioned at the surface of the cell. The monitoring of the grating was performed by means of a He−Ne laser operating at 632.8 nm. The intensity of the final first-order diffracted beam, I_1, was measured in the absence of the mask. The diffraction efficiency was calculated as $\eta = I_1/I_{tot}$, where I_{tot} was the total intensity corresponding to the sum of the transmitted and the diffracted multiple-order beams.

Homogeneous irradiation was also performed either at 488 (laser irradiation with an intensity of 25 mW cm^{-2}) or at 546 nm (conventional irradiation by using a monochromator with an intensity of 5 mW cm^{-2}).

Infrared mapping was performed on a Nicolet 6700 equipped with a Nicolet Continuμm microscope by Thermo Fisher Scientific (liquid-nitrogen-cooled MCTA detector; 128 summations). The scanning increments along the longitudinal and transversal directions were 25 and 45 μm, respectively. UV−visible spectra were recorded on a Shimadzu UV-2101 PC spectrophotometer. Fluorescence emission spectra were collected in response to the excitation at 400 nm by a Perkin−Elmer LS55 spectrophotometer.

The photofluorescence microscopy image and the 3D fluorescence profile were performed on an Olympus U6000 fluorescence microscope equipped with the filter V furnished by Olympus. The filter allowed excitation at 405 nm and partially prevented the emission between 455 and 500 nm and totally cut the ones below 455 nm.

Results and Discussion

Mechanism of Initiation of Photopolymerization for a Three-Component Sensitizer. The recording of polymer gratings without and with QDs, under a laser beam at 488 nm, implied the polymerization of the acrylate monomer mixture. Thus, it was of fundamental importance to study in detail the initiation process of the host, which involved the three-component photosensitizer in order to determine the contribution of each species in the mechanism of initiation. For this purpose, the fate of eosin Y was followed by UV−visible spectroscopy. In the absence or the presence of QDs, a drastic fall of the eosin absorption band at 542 nm occurred (Figure 1a). An absorption at approximately 400 nm developed in parallel. It was verified that in the absence of eosin, such a band was not formed. The kinetic evolution showed that this absorbance increased, reached a plateau, and, at longer irradiation time, slowly decreased (inset Figure 1a).

In order to understand the origin of the growing absorption at around 400 nm and the role of each species in the polymerization process, some experiments were carried out on 2EEEA only. With this monofunctional monomer, no network can be formed upon exposure, and therefore, the migration of the reactive species will not be prevented. Because only the initiation process was of interest, the following few experiments were undertaken in the absence of the nanoparticles (indeed, the same changes in the UV−visible spectra were observed with and without QDs).

It was first verified that the irradiation of 2EEEA at 488 nm in the presence of the three-component photosensitizer led to the formation of the absorption at roughly 400 nm. The kinetic evolution of this band was identical to the one observed in the case of the mixture of monomers. Second, it was verified if the formation of this band did not depend on the wavelength of illumination. For this purpose, the irradiation of the syrup (only with the monomer 2EEEA) was performed at the 546 nm

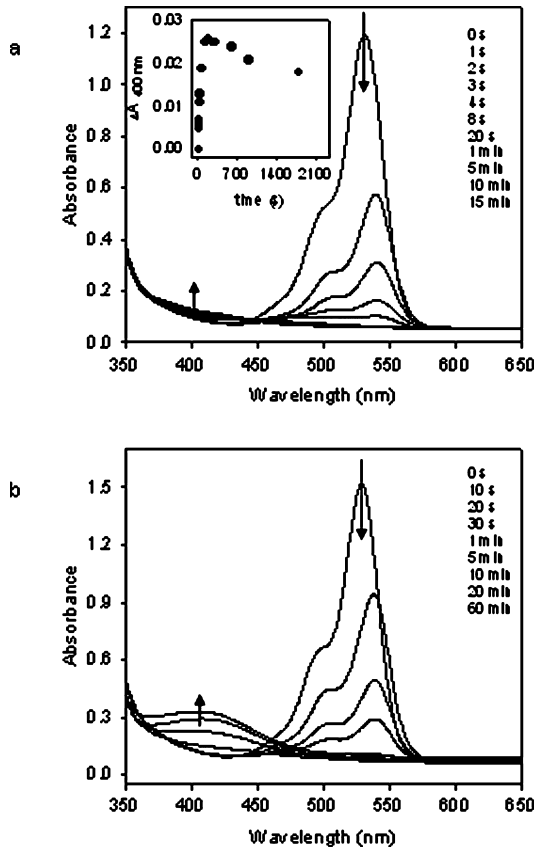

Figure 1. Evolution of the UV−visible spectra upon the irradiation of (a) the mixture of photopolymerizable acrylate monomers at 488 nm (laser irradiation) and (b) the mixture containing only the 2EEEA, eosin Y, EDMABzt, and CBr_4 at 546 nm (conventional irradiation). Inset: Kinetic evolution of the band at 400 nm.

wavelength that is in the absorption band of the dye. The exposure at 546 nm (conventional irradiation at 5 mW cm^{-2}) allowed clear evidence of the formation of a band centered at 400 nm (Figure 1b). To test the stability of the compound that is responsible for the absorption at 400 nm, the sample was then submitted to an illumination at 434 nm, and after a few minutes in such irradiation conditions, the absorbance of the band decreased. Such decay indicated the photochemical transformation of the species.

In contrast, when 2EEEA was irradiated at 546 nm in the presence of eosin Y and amine only, the band at 400 nm was not detected. The decay of eosin was slower than the one observed in the presence of the three-component photosensitizer. The photopolymerization still occurred, and the initiation reaction resulted from a photoredox process between the amine and the dye in its triplet excited state (^{3}eosin*) obtained after intersystem conversion (ISC). Lougnot et al. have studied the polymerization of dipentaerythritolpentaacrylate (DPEPA) and 2-hydroxyethyl-2-oxoazolidone acrylate monomers with a three-component photosensitizer and, in particular, the influence of the presence of heavy atoms in the triplet quantum yield of the dye, Φ_T.[35] They pointed out that the presence of CBr_4 induced an increase of Φ_T, which could explain the fast decrease of eosin observed in the case of the three-component photosensitizer. Without CBr_4, after 20 min of irradiation, 15% of the monomer was consumed, whereas with CBr_4, the same decay was obtained after only 1 min. This difference was ascribed to the presence of CBr_4, which led to a very significant improvement of photospeed.[35]

When the monomer was irradiated at 546 nm in the presence of eosin Y and CBr_4 and after the complete disappearance of the dye's absorption band, no band at 400 nm was formed, but a rather broad absorption band centered at 480 nm (with two shoulders at 452 and 512 nm) was formed (will be described later). Therefore, the compound absorbing at 400 nm could only be obtained when the amine and tetrabromomethane were both present in the photopolymerizable media. To explain the decrease of the dye, we referred to the work of Popielarz et al.[36] They were interested in studying the initiation efficiency of the eosin/co-initiator system and, in particular, eosin/CBr_4. They mentioned an electron transfer between the excited state of the dye and CBr_4, and they revealed that the efficiency depended on the stability of the radical ion pair.[36] The formed radical ion pair underwent Br^- ion transfer to the eosin radical cation, and a cage escape occurred. The bromide anion resulted from the spontaneous decomposition of the radical anion $CBr_4^{\bullet -}$ into $CBr_3^\bullet$ and Br^-.[37] By infrared spectroscopy, no significant evolution of the monomer band at 3037 cm^{-1} was observed. From this result and under our experimental conditions, it could be concluded that $CBr_3^\bullet$ radicals were not efficient enough to initiate a polymerization process.

To have a better understanding of the origin of the species absorbing at 480 nm (the broad absorption band), the following experiments were performed in acetonitrile first without the monofunctional monomer 2EEEA and second with the monomer. The UV−visible analysis of a solution of acetonitrile containing only eosin Y and tetrabromomethane revealed a partial or a complete conversion of the dye into a species that presented a spectrum identical to the one observed in the experiment described above (Figure 2a). In this case, the material solution became orange−brown. This conversion, observed at ambient temperature, could also occur when the dye was irradiated either at 488 or 546 nm. Fluorescence spectroscopy revealed a drastic decrease of the fluorescence intensity of eosin Y at 585 nm in the presence of CBr_4. Moreover, when the orange−brown solution was diluted, the color turned to pink. This color change indicated that this species was not stable, and a release of the dye occurred. Such release was confirmed by UV−visible analysis. These features suggested that the dye might exist in either a free or a complexed form by addition of CBr_4. The complexation could be described by eq 1.

$$\text{eosin} + CBr_4 = (\text{eosin}-CBr_4) \qquad (1)$$

Figure 2b represents the UV−visible spectrum of a solution of the monomer (2EEEA) and the three-component photosensitizer in acetonitrile. It showed that before irradiation at 488 nm, the dye existed in its complexed form. After exposure, the corresponding absorption band at 480 nm decreased. When the decrease reached a constant value, then the band at roughly 400 nm developed (Figure 2c). It is worth mentioning that in the absence of amine, not only the initial rate of consumption of eosin was strongly slowed down, but also, even after the complete disappearance of eosin, the band at 400 nm was not formed. Thus, the amine not only favored the dissociation of the complex but was also essential for the formation of the compound absorbing at 400 nm.

It was reported in the literature that the formation of a charge-transfer complex between the amine and CBr_4 in the ground state was characterized by a broad absorption band peaked at approximately 400 nm.[38−41] The excitation of the complex gave rise to electron transfer from the amine group to acceptor CBr_4. By taking into account the formation of a donor−acceptor

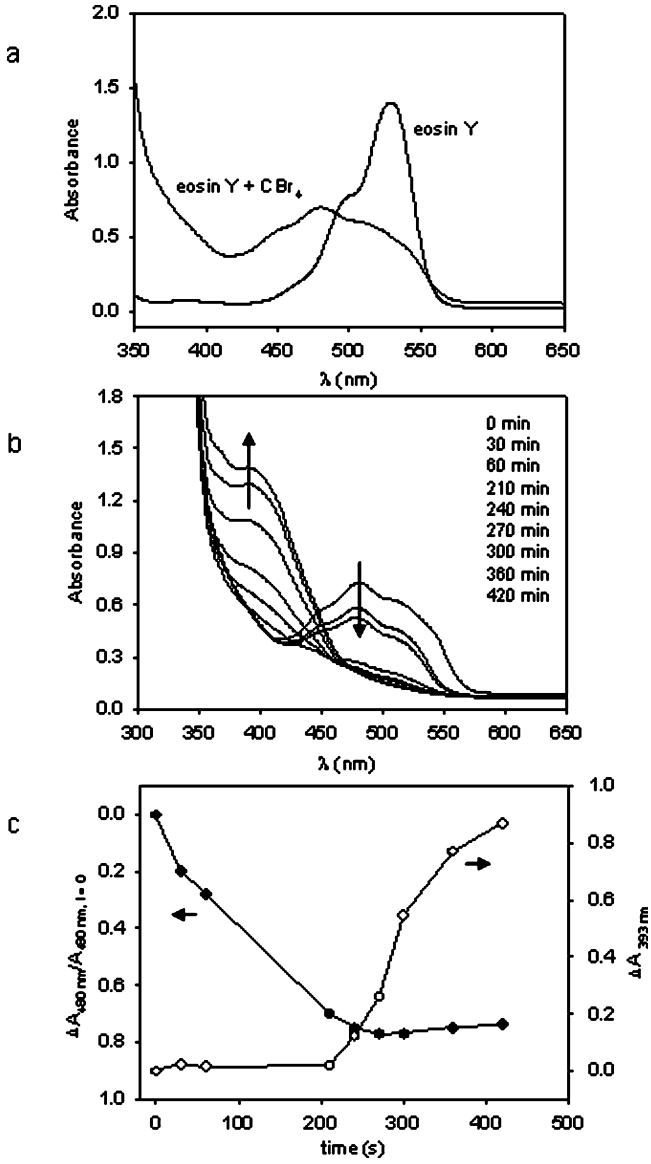

Figure 2. (a) UV−visible spectra of a solution of acetonitrile containing eosin Y in the absence and in the presence of CBr_4. (b) Evolution of the UV−visible spectra of a solution of acetonitrile containing 2EEEA, eosin Y, EDMABzt, and CBr_4 upon homogeneous irradiation at 488 nm (conventional irradiation). (c) Kinetic evolution of the decay of the band at 488 nm and of the formation of the band at 393 nm.

complex and from the results obtained above, the following mechanism of initiation of polymerization for a three-component photosensitizer can be proposed (see Scheme 1).

Eosin Y in the triplet excited state reacts with either CBr_4 or the amine EDMABzt. With the first species, the electron-transfer process gives rise to the formation of the radical anion $CBr_4^{\bullet -}$, which decomposes into the Br^- anion and $CBr_3^\bullet$ radical unable to initiate the polymerization. Upon irradiation, eosin reacts with tetrabromomethane, which leads to a compound absorbing at 480 nm. This species acts as an intermediate in the initiation process. However, it rapidly dissociates in the presence of amine. We could suppose that due to the polymerization, the viscosity of the media increases and may favor the vicinity of the species. This fact may explain that the released CBr_4 could form a charge-transfer complex with the amine (absorbing at 400 nm). Then, the excitation of the charge-transfer complex would give rise to the formation of $EDMABzt^{\bullet +}$ and $CBr_4^{\bullet -}$ by an electron

SCHEME 1: Mechanism of Initiation of Photopolymerization for a Three-Component Sensitizer

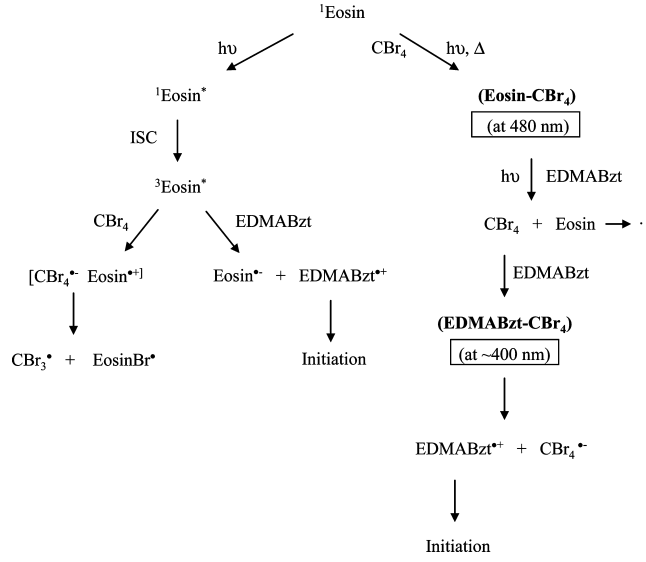

transfer from the amine group to tetrabromomethane. The radical cations could initiate the polymerization. With the amine, a typical photoredox process implying eosin Y in the triplet excited state and the amine occurs.

Influence of CdSe/ZnS QDs in the Polymerization Process. ***Recording of Pure Polymer Gratings.*** The kinetic evolution of the diffraction efficiency, η, of the gratings recorded in the basic composition of pure polymer (without QDs) is represented in Figure 3a as a function of irradiation time at various writing intensities.

For all recording intensities, during the first 3 s of exposure, a decrease of η was observed (not shown in Figure 3a). Such behavior was attributed to the presence of the amplitude mask. Indeed, it must be noticed that the grating recording and the dynamic measurement of the diffracted first-order intensity, I_1, were preformed through the amplitude mask composed of dark and transparent lines, which was placed at the top of the sample. It was then verified that when the mask was distanced from (but still imaged on) the sample (to monitor only the photopolymer grating but not the amplitude mask), the decrease was not observed. That is why this initial part is not shown in Figure 3a. After the first 3 s, η increased and reached a plateau. In general, the higher the writing intensity was, the higher the maximum value of η was. However, above 35 mw cm^{-2}, the attained value at the plateau started to decrease. To have better insight into the influence of the laser intensity, the final (established) diffraction efficiency η was measured in the absence of the mask for each recording intensity. Table 1 shows that η depended on the laser intensity in a nonmonotone way; it increased and passed through a maximum for a recording intensity of 35 mW cm^{-2}.

From those diffraction efficiency values, the refractive index modulation could be estimated by using the following equation[42]

$$\eta \approx \sin^2\left(\frac{\pi \Delta n d}{\lambda}\right) \qquad (2)$$

where Δn is the refractive index modulation depth, d is the thickness of the film, and λ is the wavelength of the measuring light. The monitoring was performed at nearly normal incidence. The corresponding results are also reported in Table 1. It must

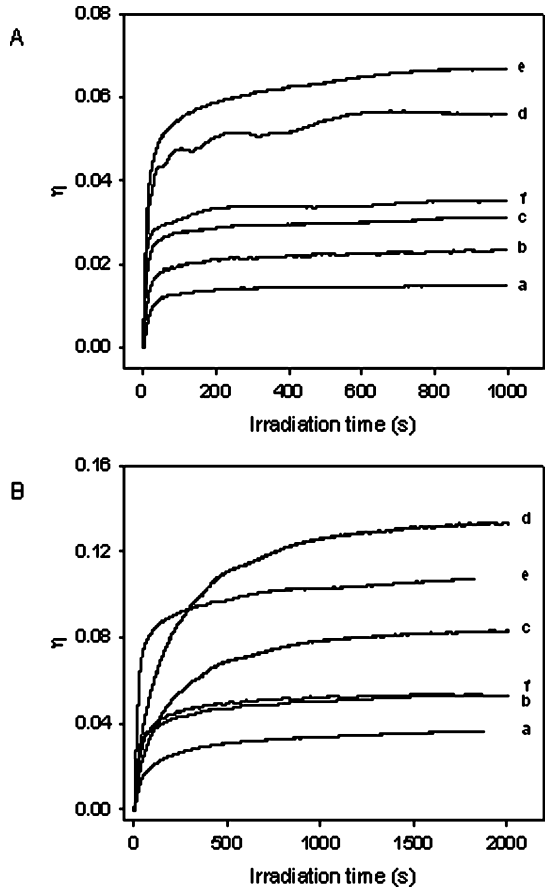

Figure 3. Kinetic evolution of the diffraction efficiency, η, of the gratings recorded (A) in pure acrylate monomer mixture and (B) in QD dispersed acrylate monomer mixture (0.5 wt % of QDs) at 488 nm with the intensity range of 10−40 mW cm^{-2}: (a) 10, (b) 20, (c) 25, (d) 30, (e) 35, and (f) 40 mW cm^{-2}.

TABLE 1: Established Diffraction Efficiency and Refractive Index Modulation of Gratings Recorded in Pure Acrylate Monomers As a Function of Recording Intensity

intensity (mW cm^{-2})	fiffraction efficiency (%)	$\Delta n \times 10^3$
10	1.5 ± 0.1	2.25 ± 0.08
20	2.34 ± 0.02	2.81 ± 0.01
25	3.1 ± 0.1	3.24 ± 0.05
30	5.59 ± 0.06	4.37 ± 0.02
35	6.67	4.78
40	3.5 ± 0.2	3.45 ± 0.1

be mentioned that given the geometrical parameters of our experiment (the factor Q is small) and the low diffraction efficiency (the modulation depth is also very small), one could use the diffraction efficiency of "thin and weak" gratings, expressed by Bessel functions. However, given the very small modulation depth, the approximation used in the paper gave approximately the same results. It can be seen in Table 1 that Δn attained a maximum value of 4.78 × 10^{-3}, corresponding to a recording intensity of 35 mW cm^{-2}. According to the literature, larger refractive index modulations were difficult to obtain for pure polymer materials.[24]

Recording of QD Dispersed Polymer Gratings. The kinetic evolution of the diffraction efficiency of the gratings recorded in QD dispersed polymer (with 0.5 wt % of QDs) is represented in Figure 3b as a function of the writing intensity; η increased and reached a plateau with an evolution similar to the one obtained in the absence of QDs.

TABLE 2: Established Refractive Index Modulation of Gratings Recorded in 0.5 wt % QD Dispersed Acrylate Monomers As a Function of Recording Intensity

intensity (mW cm^{-2})	diffraction efficiency (%)	$\Delta n \times 10^3$
10	3.64 ± 0.06	3.52 ± 0.03
20	5.3 ± 0.1	4.26 ± 0.05
25	8.27 ± 0.04	5.34 ± 0.02
30	13.2 ± 0.5	6.8 ± 0.1
35	10.7 ± 0.4	6.1 ± 0.1
40	5.34 ± 0.09	4.27 ± 0.04

From the comparison of Tables 1 and 2, it appears that a relatively weak amount of QDs was sufficient to modify noticeably the diffraction efficiency of the grating. Thus, the maximum value of η increased from 6.67% in pure photopolymer to 13.2% in the nanoparticle-based matrix. By applying eq 2, the corresponding refractive index modulation was determined. Table 2 reveals that Δn increased by a factor of 1.4 by the addition of 0.5 wt % of QDs, achieving the value of Δn of 6.8 × 10^{-3} compared to 4.8 × 10^{-3} in pure polymer.

To have better insight into the polymer and QDs distribution and into the QDs diffusion process, the grating was analyzed both by infrared microspectrophotometry and by fluorescence microscopy. Infrared mapping allowed examination, in detail, of the spatial distribution of the polymer as a function of the irradiation time inside of the dark and transparent fringes.

Figure 4a shows a periodic distribution of the formed polymer characterized by the band at 2945 cm^{-1} (as discussed later). Indeed, after 10 min of grating recording, the polymer concentration was higher in the irradiated zones and minimum in the dark zones. This result was consistent with the previous density distribution of the polymer measured by Raman spectroscopy.[14,20] However, at longer irradiation time, such as 20 min, the profile of polymerization was less pronounced (by a factor of roughly

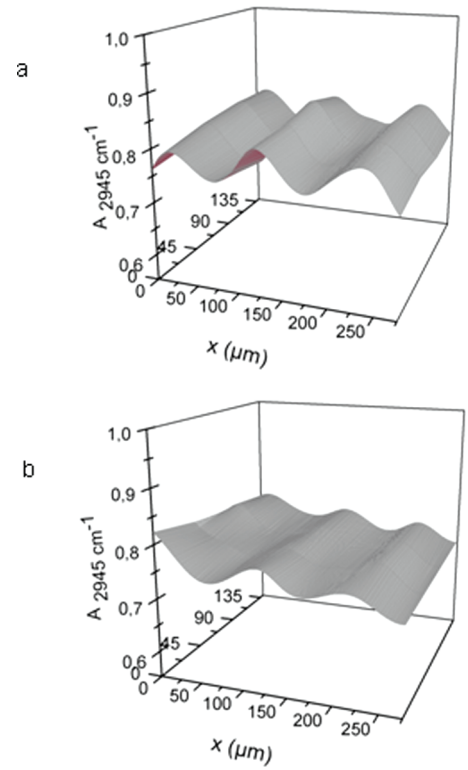

Figure 4. Infrared mapping of the formed polymer (band at 2940−2945 cm^{-1}) for gratings recorded in QD dispersed photopolymer after (a) 10 and (b) 20 min of irradiation at 30 mW cm^{-2}.

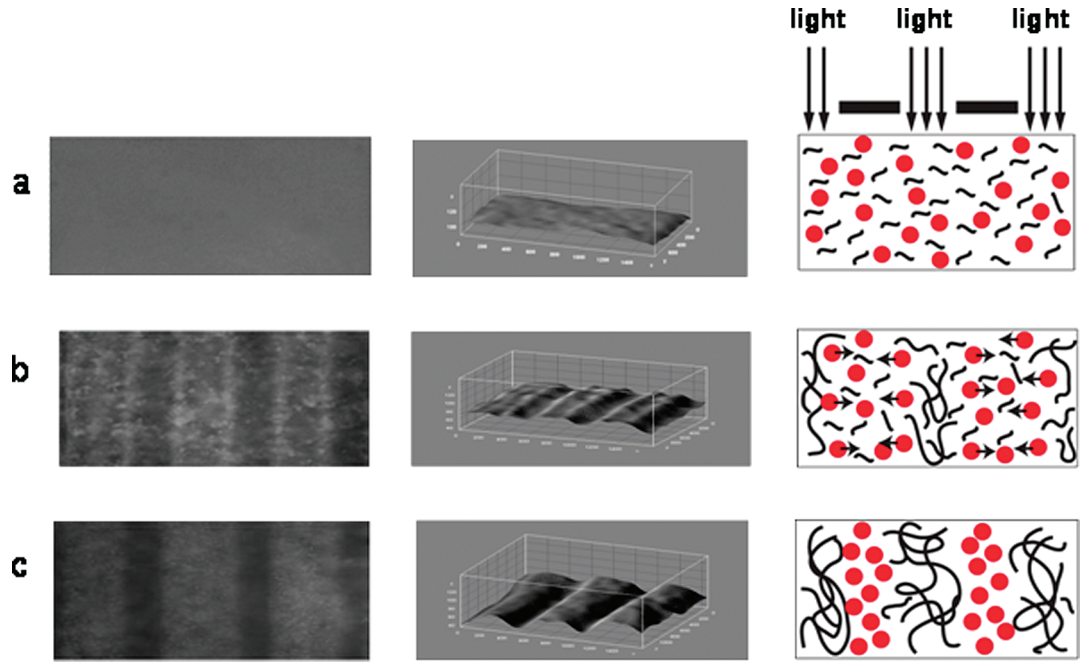

Figure 5. Photofluorescence microscopy image (left), 3D fluorescence profile (middle), and schematic representation (right) of QD dispersed acrylate photopolymer (a) before irradiation and (b) after 10 and (c) 20 min of irradiation at 30 mW cm^{-2}.

2) compared to that obtained after 10 min of exposure (Figure 4b). This feature evidenced the propagation of the polymerization in the dark zones at longer irradiation time.

In parallel, for the first time to our knowledge, the spatial diffusion of nanoparticles was monitored by fluorescence microscopy upon hologram recording time. In some studies,[7,8] this technique was used as a probe of the movement of the photoluminescent nanoparticles, but only when the steady-state value of the diffraction efficiency was achieved. It was first verified that the emitted fluorescence was due to the QDs. Indeed, after one minute of homogeneous irradiation, in response to the excitation at 400 nm, the fluorescence intensity of eosin Y was negligible compared to that of the nanoparticles (band at 620 nm). This latter slightly decreased and remained constant after 5 min of exposure.

Back to the periodic excitation case, initially, the QDs were homogeneously dispersed in the monomer syrup (Figure 5a). Figure 5b revealed that after 10 min of exposure, the nanoparticles were pushed from the illuminated zones to the interface of the irradiated and nonirradiated zones, where the light intensity gradient is maximal. Thus, the fluorescence profile presented two maxima centered at each side of the bright fringes. Obviously, the single spatial frequency *sin*-like approximation of refractive index modulation is no more accurate here, and higher spatial frequencies must be taken into account for the grating description. At longer irradiation time (20 min), QDs were concentrated at the middle of the dark zones (Figure 5c), as pointed out by the fluorescence profile. From these features, a scheme representing the diffusion process upon irradiation time was given in Figure 5 (right column). It is well-known that the propagation of the polymerization into the dark zones leads to a decrease of the refractive index modulation depth and consequently of the diffraction efficiency. However, this decrease is counterbalanced by an increase of the concentration of QDs in the dark fringes, which provides an enhancement of the refractive index modulation. These two concomitant phenomena permitted explaination of why once the plateau was reached, the diffraction efficiency was maintained constant during the first 30 min of recording (not shown).

At the same time, higher recording intensities should favor the fast polymerization and therefore the formation of a denser network. However, this latter would limit the diffusion of QDs. Higher exposure intensities should also provoke the polymerization into the nonilluminated zones. Both phenomena would decrease the refractive index modulation depth, which explains its nonmonotone dependence upon the exposure intensity (Table 2).

In the case of gold-nanoparticle-containing composites, on the basis of in situ infrared spectroscopy, Stumpe et al.[11] pointed out that even at low loading (1.5%), these nanoparticules were not only involved in the diffusion process but also played a role in the kinetics of photopolymerization. One could ask if in our case, the QDs influenced the polymerization of the two-monomer nanocomposites as in the case of gold particles. For this purpose, we have monitored the fate of eosin Y and the vinylic groups of the acrylate monomers without and with QDs (1% QDs loading) by using UV−visible and infrared spectroscopy under homogeneous exposure at 488 nm with a power of 25 mW cm^{-2}, which corresponded to the intensity ranges of our grating recording. The decay of eosin Y was defined as $(A_0 - A_t)/A_0$, where A_0 and A_t represent the absorbance of the band at 542 nm before irradiation and at a given irradiation time t, respectively. The kinetic evolution of eosin decay plotted in Figure 6 highlighted that the presence of the nanoparticles affected the consumption rate of the dye. Indeed, the initial rate fell down by a factor of 5 when QDs were added in the media.

The evolution of the infrared spectra in the 3060−2900 cm^{-1} domain upon irradiation shows a decrease of the band at 3037 cm^{-1}, which is attributed to the CH═CH bonds,[43] and, at the same time, an increase of a band at 2940 cm^{-1}, which is assigned to the methylene groups arising from the polymerization of the vinylic functions. Such assignement was confirmed by the linear correlation between the formation of the band at 2940 cm^{-1} and the consumption of the CH═CH absorption band (inset Figure 7). The same features were observed in the case of QD dispersed composites.

The comparison of the kinetic evolution of the conversion of the monomers in the absence and in the presence of QDs

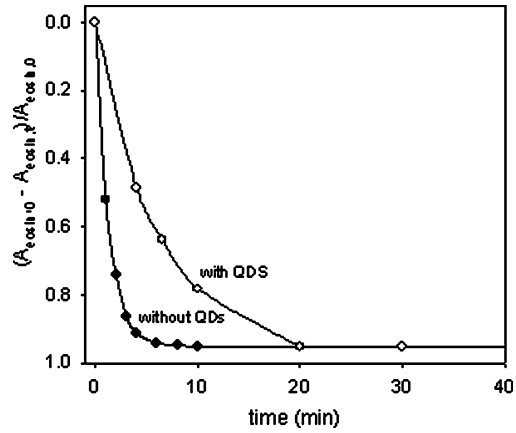

Figure 6. Kinetic evolution of the decay of eosin Y (band at 542 nm) in a monomer mixture without and with 0.5% of QDs upon homogeneous exposure at 488 nm.

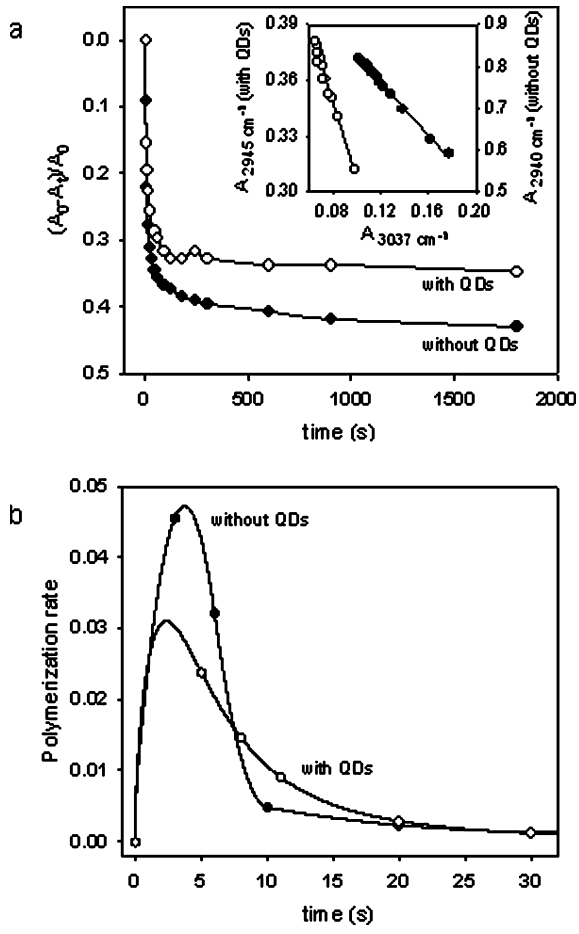

Figure 7. (a) Kinetic evolution of the decay of the CH=CH groups (band at 3037 cm^{-1}) in the monomer mixture without and with 1% of QDs upon homogeneous exposure at 488 nm. Inset: Correlation between the decrease of the C−H bonds of the vinyl groups (band at 3037 cm^{-1}) and the formation of the CH_2 groups (band at 2940 cm^{-1}). (b) Polymerization rate in the monomer mixture without and with 1 wt % of QDs.

highlighted the role played by the QD nanoparticles even at relatively low loading (1%) (Figure 7b). The conversion of the monomers did not exceed 35% in the presence of 1 wt % of QDs, compared to 43% in the absence of QDs. The double bonds could not undergo a complete conversion because the reactive macroradicals were trapped in the tridimensional network. To get better insight into the influence of QDs in the kinetics, the rate of polymerization was determined in each case. This later was calculated from d(conversion)/dt (Figure 7c).

The polymerization rate was the highest for the pure monomer mixture. It strongly decreased when the media contained QDs. Therefore, the QD nanoparticles contributed both to the diffusion process (triggered by the photopolymerization) and to the change in the kinetics of polymerization. With the decrease of the polymerization rate, the media underwent a smaller increase of the viscosity, which favored the diffusion of monomers and nanoparticles during grating recording. This feature contributes to enhance the refractive index modulation and therefore the diffraction efficiency.

Conclusions

First, particular attention was given to the initiation step of the polymerization of the host matrix for the three-component photosensitizer (eosin Y, amine EDMABzt, and CBr_4). From a physicochemical study, a mechanism of initiation which involved each component of the sensitizer system was proposed.

Then, we were interested in refractive index modulation gratings recorded in the acrylate monomers' mixture. The dispersion of 0.5% QDs in the monomer syrup provided a significant enhancement of the refractive index modulation Δn from 4.8×10^{-3} to 6.8×10^{-3}. This increase was ascribed not only to the diffusion of the monomers but also to the counter diffusion of the nanoparticles. The infrared microspectroscopy revealed that the polymerization propagated and proceeded inside of the dark zones at longer exposure times. The fluorescence microscopy showed that upon the grating recording time, the nanoparticles were first pushed at the interface of the bright and dark zones and then concentrated in the middle of the nonirradiated areas.

Finally, homogeneous laser irradiation allowed determination of the contribution of QDs in the polymerization process. It was shown that the nanoparticles were not inert and noticeably influenced the kinetics, giving rise to a decrease of the rate of consumption of eosin and of the polymerization rate. This latter favored the diffusion of monomers and the QDs and thus contributed to the increase of Δn.

Many questions remain still to be answered. Thus, one could ask about the efficiency of QDs to photoinitiate the polymerization of the acrylate mixture in the absence of a photosensitizer. In the same way, it is of fundamental importance to gain further understanding of the decrease of the polymerization rate in the presence of the QDs. The work is still in progress, and the results will be presented in the next study.

Acknowledgment. Professor M. Sarakha and Doctor P. Wong-Wah-Chung are gratefully acknowledged for helpful discussion. The Natural Sciences and Engineering Research Council of Canada (NSERC) and the Canadian Institute for Photonic Innovations are thanked for the financial support.

References and Notes

(1) Paquet, C.; Kumacheva, E. *Mater. Today* **2008**, *11*, 48–56.
(2) Gu, C.; Xu, Y.; Liu, Y.; Pan, J. J.; Zhou, F.; He, H. *Opt. Mater.* **2003**, *23*, 219–227.
(3) Beecroft, L. L.; Ober, C. K. *Chem. Mater.* **1997**, *9*, 1302–1317.
(4) Hide, F.; Díaz-García, M. A.; Schwartz, B. J.; Heeger, A. J. *Acc. Chem. Res.* **1997**, *30*, 430–436.
(5) Wong, W. H.; Liu, K. K.; Chan, K. S.; Pun, E. Y. B. *J. Cryst. Growth* **2006**, *288*, 100–104.
(6) Barachevskii, V. A. *High Energy Chem.* **2006**, *40*, 131–141.
(7) Sakhno, O. V.; Goldenberg, L. M.; Stumpe, J.; Smirnova, T. N. *J. Opt. A: Pure Appl. Opt.* **2009**, *11*, 0204013–0204025.
(8) Sakhno, O. V.; Smirnova, T. N.; Goldenberg, L. M.; Stumpe, J. *Mater. Sci. Eng., C* **2008**, *28*, 28–35.

(9) Ninjbadgar, T.; Garnweitner, G.; Börger, A.; Goldenberg, L. M.; Sakhno, O. V.; Stumpe, J. *Adv. Funct. Mater.* **2009**, *19*, 1–7.
(10) Vaia, R. A.; Dennis, C. L.; Natarajan, L. V.; Tondiglia, V. P.; Tomlin, D. W.; Bunning, T. J. *Adv. Mater.* **2001**, *13*, 1570–1574.
(11) Goldenberg, L. M.; Sakhno, O. V.; Smirnova, T. N.; Helliwell, P.; Chechik, V.; Stumpe, J. *Chem. Mater.* **2008**, *20*, 4619–4627.
(12) Balan, L.; Turck, C.; Soppera, O.; Vidal, L.; Lougnot, D. J. *Chem. Mater.* **2009**, *21*, 5711–5718.
(13) Smirnova, T. N.; Sakhno, O. V.; Bezrodnyj, V. I.; Stumpe, J. *Appl. Phys. B* **2005**, *80*, 947–951.
(14) Sánchez, C.; Escuti, M. J.; van Heesch, C.; Bastiaansen, C. W. M.; Broer, D. J.; Loos, J.; Nussbaumer, R. *Adv. Funct. Mater.* **2005**, *15*, 1623–1629.
(15) Suzuki, N.; Tomita, Y.; Kojima, T. *Appl. Phys. Lett.* **2002**, *81*, 4121–4123.
(16) Suzuki, N.; Tomita, Y. *Appl. Phys. Lett.* **2006**, *88*, 011105/1–011105/3.
(17) Suzuki, N.; Tomita, Y. *Appl. Opt.* **2004**, *43*, 2125–2129.
(18) Tomita, Y.; Suzuki, N.; Chikama, K. *Opt. Lett.* **2005**, *30*, 839–841.
(19) Tomita, Y.; Chikama, K.; Nohara, Y.; Suzuki, N.; Furushima, K.; Endoh, Y. *Opt. Lett.* **2006**, *31*, 1402–1404.
(20) Chikama, K.; Mastubara, K.; Oyama, S.; Tomita, Y. *J. Appl. Phys.* **2008**, *103*, 113108/1–113108/6.
(21) Suzuki, N.; Tomita, Y.; Ohmori, K.; Hidaka, M.; Chikama, K. *Opt. Express* **2006**, *14*, 12712–12719.
(22) Ostrowski, A. M.; Naydenova, I.; Toal, V. *J. Opt. A: Pure Appl. Opt.* **2009**, *11*, 034004–034007.
(23) Leite, E.; Naydenova, I.; Pandey, N.; Babeva, T.; Majano, G.; Mintova, S.; Toal, V. *J. Opt. A: Pure Appl. Opt.* **2009**, *11*, 024016–024024.
(24) Sakhno, O. V.; Goldenberg, L. M.; Stumpe, J.; Smirnova, T. N. *Nanotechnology* **2007**, *18*, 105704–105711.
(25) Li, X.; Chon, J. W. M.; Gu, M. *Aust. J. Chem.* **2008**, *61*, 317–323.
(26) Garnweitner, G.; Goldenberg, L. M.; Sakhno, O. V.; Antonietti, M.; Niederberger, M.; Stumpe, J. *Small* **2007**, *3*, 1626–1632.
(27) Kojima, T.; Tomita, Y. *Opt. Rev.* **2002**, *9*, 222–226.
(28) Karpov, G. M.; Obukhovsky, V. V.; Smirnova, T. N.; Lemeshko, V. V. *Opt. Commun.* **2000**, *174*, 391–404.
(29) Tomita, Y.; Suzuki, N.; Furushima, K.; Endoh, Y. Organic Holographic Materials and Aplications III. *Proc. SPIE* **2005**, *5939*, 593909/1–593909/9.
(30) Kim, W. S.; Jeong, Y.-C.; Park, J.-K. *Appl. Phys. Lett.* **2005**, *87*, 012106/1–012106/3.
(31) Kim, W. S.; Jeong, Y.-C.; Park, J.-K. *Opt. Express* **2006**, *14*, 8967–8973.
(32) Lee, S.; Jeong, Y.-C.; Heo, Y.; Kim, S. I.; Choi, Y.-S.; Park, J.-K. *J. Mater. Chem.* **2009**, *19*, 1105–1114.
(33) Ling, F.; Dan, L.; Zhou, H.; Yao, J. Q. *Opt. Mater.* **2008**, *31*, 206–208.
(34) Barichard, A.; Mailhot, B.; Rivaton, A.; Israëli, Y.; Galstian, T. *Nanotechnology* **2009**, *20*, 255303–255306.
(35) Noiret, N.; Meyer, C.; Lougnot, D. J. *Pure Appl. Opt.* **1994**, *3*, 55–71.
(36) Popielarz, R.; Vogt, O. *J. Polym. Sci., Part A: Polym. Chem.* **2008**, *46*, 3519–3532.
(37) Tikhomirov, V. A.; German, E. D. *J. Electroanal. Chem.* **1998**, *450*, 13–20.
(38) Erddalane, A.; Fouassier, J. P.; Morlet-Savary, F.; Takimoto, Y. *J. Polym. Sci., Part A: Polym. Chem.* **1996**, *34*, 633–642.
(39) Vannikov, A. V.; Grishina, A. D.; Pereshivko, L.Ya.; Krivenko, T. V.; Savelyev, V. V.; Kostenko, L. I.; Rychwalski, R. W. *J. Photochem. Photobiol., A* **2002**, *150*, 187–194.
(40) Fouassier, J.-P.; Erddalane, A.; Morlet-Savary, F.; Sumiyoshi, I.; Harada, M.; Kawabata, M. *Macromolecules* **1994**, *27*, 3349–3356.
(41) Budyka, M. F. *J. Photochem. Photobiol., A* **1995**, *88*, 15–18.
(42) Kogelnick, H. *Bell Syst. Tech. J.* **1969**, *48*, 29096.
(43) Avram, M.; Mateescu, G. D. *Spectroscopie Infrarouge*; Dunod: Paris, 1970.

JP1040713